

## Supplementary Information

# Hierarchical Peroxiredoxin Assembly Through Orthogonal pH-response and Electrostatic Interactions

Eduardo Anaya-Plaza,<sup>a\*</sup> Zülfü Özdemir,<sup>b</sup> Zdenek Wimmer,<sup>b</sup> and Mauri A. Kostiainen<sup>a\*</sup>

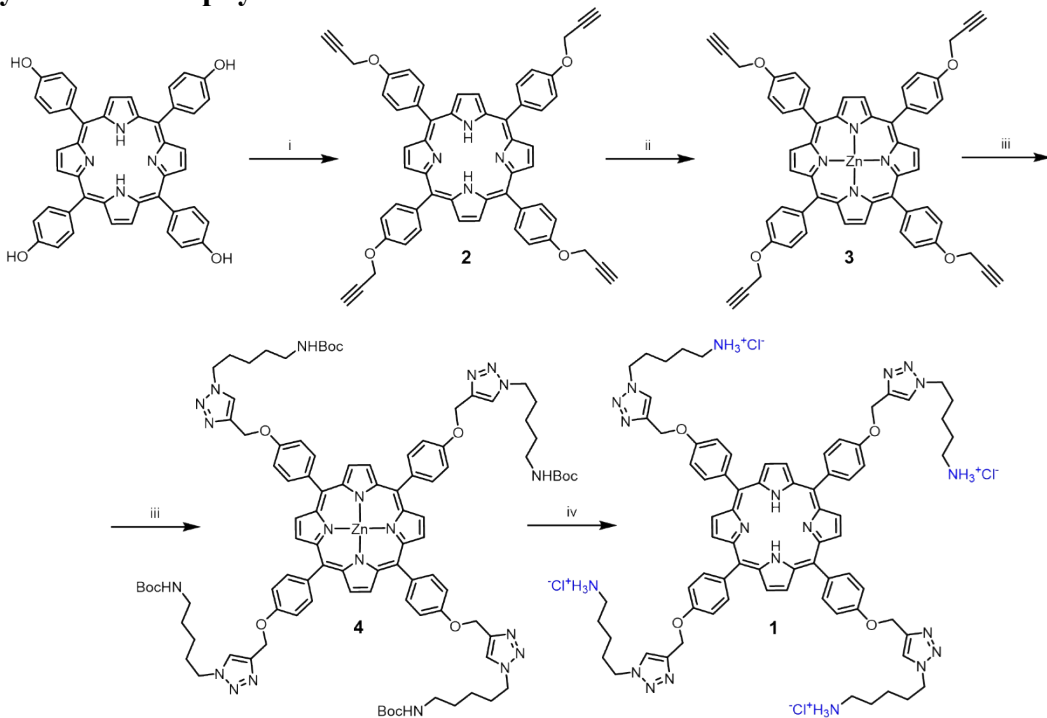
<sup>a</sup> Department of Bioproducts and Biosystems, Aalto University, P. O. Box 16100, 00760 Aalto, Finland.  
Email: [eduardo.anaya@aalto.fi](mailto:eduardo.anaya@aalto.fi); [mauri.kostiainen@aalto.fi](mailto:mauri.kostiainen@aalto.fi)

<sup>b</sup> Department of Chemistry of Natural Compounds, University of Chemistry and Technology in Prague,  
Technická 5, 16628 Prague 6, Czech Republic.

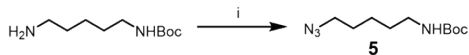
## **1 Table of contents**

<b>1</b>	<b>Table of contents.....</b>	<b>S2</b>
<b>2</b>	<b>Synthesis of Porphyrin 1 .....</b>	<b>S3</b>
<b>3</b>	<b>Low magnification TEM images .....</b>	<b>S4</b>
<b>4</b>	<b>Characterization of Por 1 and intermediates .....</b>	<b>S7</b>
4.1	Por 2.....	S7
4.2	Por 3.....	S8
4.3	Por 4.....	S10
4.4	Por 1.....	S11
4.5	Intermediate 5 .....	S13

## 2 Synthesis of Porphyrin 1



Scheme 1. Synthetic procedure for **4**. Reagents used: i) propargyl chloride,  $\text{K}_2\text{CO}_3$ , 4 Å molecular sieves, in toluene-DMF (2:1), under argon atmosphere, at 60°C; ii)  $\text{Zn}(\text{OAc})_2$ , in  $\text{CHCl}_3$ , rt; iii) **5**,  $\text{CuSO}_4 \cdot 5\text{H}_2\text{O}$ /TBTA, sodium ascorbate, in  $\text{DCM}/\text{H}_2\text{O}$ , rt; iv) 1.0 M HCl in EtOAc, rt.



Scheme 2. Synthetic procedure for **5**. Reagents used: i) propargyl chloride,  $\text{K}_2\text{CO}_3$ , 4 Å molecular sieves, in toluene-DMF (2:1), under argon atmosphere, at 60°C; ii)  $\text{Zn}(\text{OAc})_2$ , in  $\text{CHCl}_3$ , rt; iii) **6**,  $\text{CuSO}_4 \cdot 5\text{H}_2\text{O}$ /TBTA, sodium ascorbate, in  $\text{DCM}/\text{H}_2\text{O}$ , rt; iv) 1.0 M HCl in EtOAc, rt.

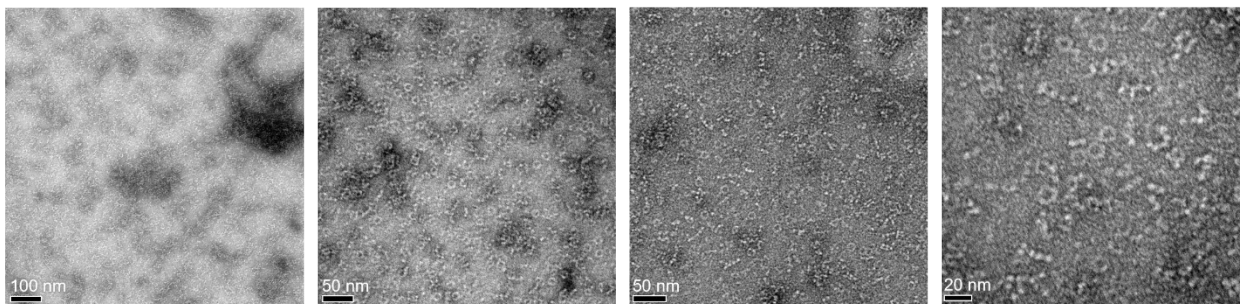
### 3 DLS data

pH 8	Volume						PDI	Intensity					
[1] (M)	Peak 1 (nm)	Area (%)	Peak 2 (nm)	Area (%)	Peak 3 (nm)	Area (%)		Peak 1 (nm)	Area (%)	Peak 2 (nm)	Area (%)	Peak 3 (nm)	Area (%)
0	11.9	98.7	2012	1.3	-	-	0.435	20.46	54.7	-	-	1973	45.3
1.3E-7	13.05	65.1	1820	1.7	0.85	33.3	0.371	17.68	38.6	875.4	46.2	4165	12.9
3.4E-7	13.5	97.9	1658	2.1	-	-	0.509	20.98	35.1	693.4	53.5	3887	11.4
6.7E-7	11.97	94.6	100.6	0.4	-	-	0.9	16.36	13.8	184	29.8	1538	56.4
1.3E-6	12.57	28.3	586	49	-	-	0.458	14.21	0.8	362.4	95.9	4661	3.3
3.4E-6	87.97	16.7	945.4	83.3	-	-	0.399	-	-	402.5	97.2	4329	2.8
6.7E-6	50.76	5.4	551.2	94.6	-	-	0.241	55.63	1	410.1	99	-	-
1.3E-5	-	-	1224	100	-	-	0.296	-	-	793.7	97.6	4625	2.4
3.4E-5	-	-	1420	97.5	-	-	0.289	203.6	3.1	1213	93.6	4917	3.3
6.7E-5	-	-	1742	100	-	-	0.227	315.4	1.5	1571	98.5	-	-
1.3E-4	-	-	2019	100	-	-	0.305	-	-	2014	100	-	-
pH 6	Volume						PDI	Intensity					
[1] (M)	Peak 1 (nm)	Area (%)	Peak 2 (nm)	Area (%)	Peak 3 (nm)	Area (%)		Peak 1 (nm)	Area (%)	Peak 2 (nm)	Area (%)	Peak 3 (nm)	Area (%)
0	19.98	90.2	698.1	9.6	85.68	0.2	0.752	23.03	14.2	535.5	83.3	102	2.1
1.3E-7	25.13	79.9	667.8	19.7	5246	0.4	0.753	34	15	516.1	83.9	5240	1
3.4E-7	22.68	78.1	950.2	20.3	4279	1.6	0.747	26.62	10.8	602.9	82.7	4151	6.5
6.7E-7	26.89	88.2	432.8	10.7	4070	1.1	0.634	29.27	16.5	342.6	80.7	4574	2.7
1.3E-6	22.58	92.1	411.4	7.8	4242	0.1	0.638	25.69	16.3	335.3	82.8	4541	0.9
3.4E-6	24.99	63.7	635.1	26	1996	9.3	0.583	30.69	6.9	611.6	90.9	5066	2.2
6.7E-6	34.2	59.8	506.5	37.8	4664	2.4	0.48	37.26	8.6	414.1	88.3	4838	3
1.3E-5	44.79	15.4	586.5	43.5	2278	41.2	0.559	48.09	5.2	861.7	94.8	0	0
3.4E-5	35.52	6.8	109.1	3.2	1063	90	0.374	2975	3.8	591.3	93.4	4866	2
6.7E-5	56.29	13.2	798.1	73.2	3762	13.6	0.464	4230	7.5	514.3	87.7	62.7	4.8
1.3E-4	-	-	963.8	98.8	5219	1.2	0.289	5226	1.4	666	98.6	0	0
pH 4	Volume						PDI	Intensity					
[1] (M)	Peak 1 (nm)	Area (%)	Peak 2 (nm)	Area (%)	Peak 3 (nm)	Area (%)		Peak 1 (nm)	Area (%)	Peak 2 (nm)	Area (%)	Peak 3 (nm)	Area (%)
0	57.7	7.3	1480	92.3	-	-	0.63	68.05	8.7	1320	89.3	172.2	1.5
1.3E-7	60.18	6.7	1500	93.1	-	-	0.601	84.2	9.1	1309	90.3	5356	0.6
3.4E-7	53.74	4	1383	96	-	-	0.309	56.84	3.6	1262	96.4	-	-
6.7E-7	-	-	1345	100	-	-	0.224	-	-	1252	100	-	-
1.3E-6	58.2	7.6	1294	92.4	-	-	0.432	61.43	7.9	1180	92.1	-	-
3.4E-6	62.13	7.4	1390	92.6	-	-	0.562	66.48	9.8	1267	90.2	-	-
6.7E-6	62.18	15.9	1232	83.3	-	-	0.915	76.25	18.4	1064	80	5332	1.6
1.3E-5	69.74	10.6	1474	89.4	-	-	0.888	80.04	18.6	1297	81.4	-	-
3.4E-5	78.39	5.6	1704	94	-	-	0.754	86.03	15	1563	84.1	5361	0.9
6.7E-5	71.46	11.1	1570	88.5	-	-	0.912	87.01	21.9	1390	77.4	5380	0.7
1.3E-4	62.56	2.4	1797	97.6	-	-	0.609	67.95	2.7	1711	85.5	67.95	2.7

Table S1. Peak position and relative area, as well as PDI for DLS measurements after volume and intensity fitting.

#### 4 Low magnification TEM images

**Prx, pH 8**



**Prx-1, pH 8**

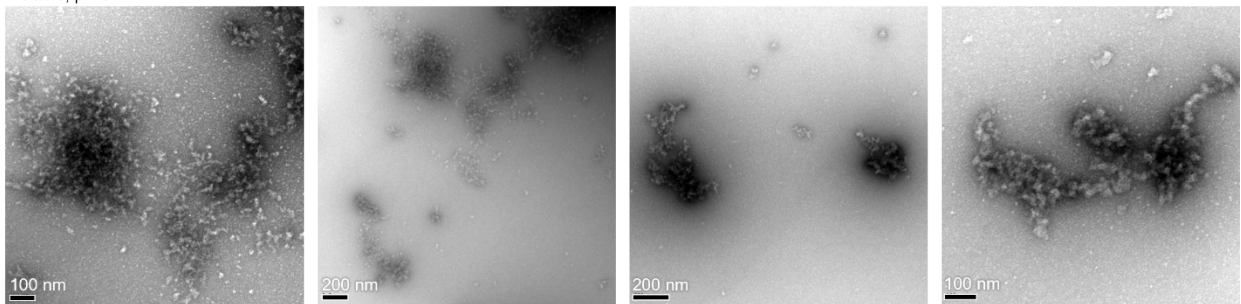
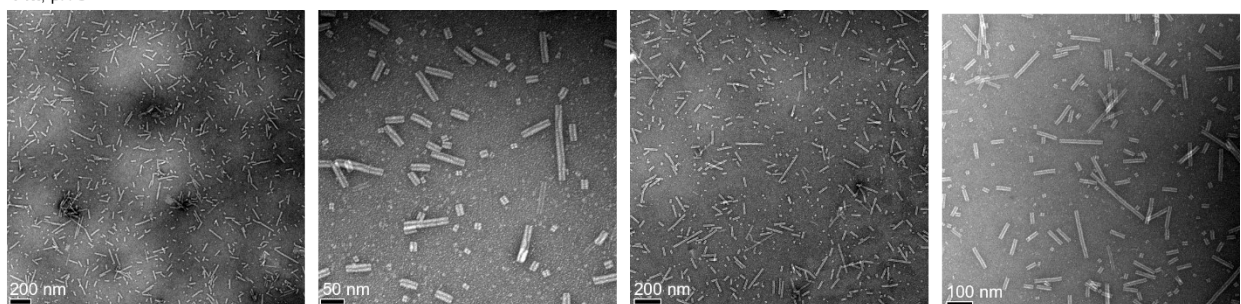


Figure S1. Additional TEM images of the **Prx** (top) and **Prx-1** complexes (bottom) at pH 8. [Prx] = 0.1 mg/mL, and [1] = 0.2 mg/mL, stained with uranyl formate 2%. As seen from the images, assembly of the **Prx** with **1** resulted in large amorphous aggregates.

**Prx, pH 6**



**Prx-1, pH 6**

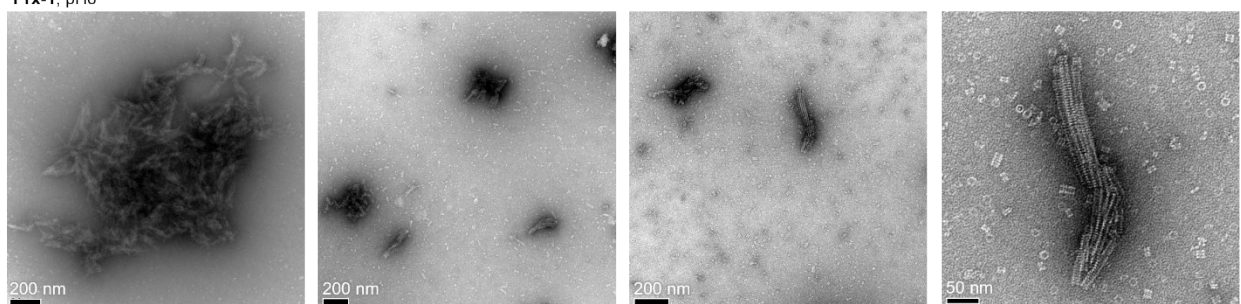


Figure S2. Additional TEM images of the **Prx** (top) and **Prx-1** complexes (bottom) at pH 6. [Prx] = 0.1 mg/mL, and [1] = 0.2 mg/mL, stained with uranyl formate 2%. As seen from the images, assembly of the **Prx** with **1** resulted in partially aligned aggregates.

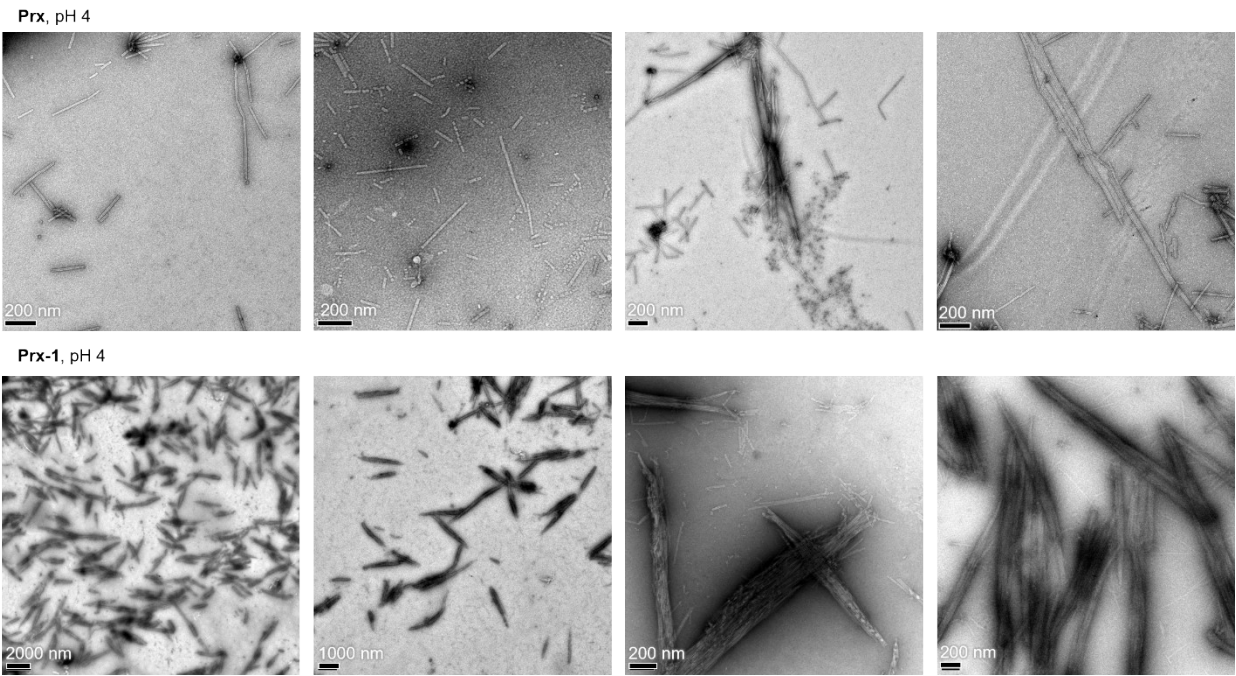


Figure S3. Additional TEM images of the **Prx** (top) and **Prx-1** complexes (bottom) at pH 6.  $[Prx] = 0.1 \text{ mg/mL}$ , and  $[1] = 0.2 \text{ mg/mL}$ , stained with uranyl formate 2%. As seen from the images, assembly of the **Prx** with **1** resulted in partially aligned aggregates.

## 5 Characterization of Por 1 and intermediates

### 5.1 Por 2

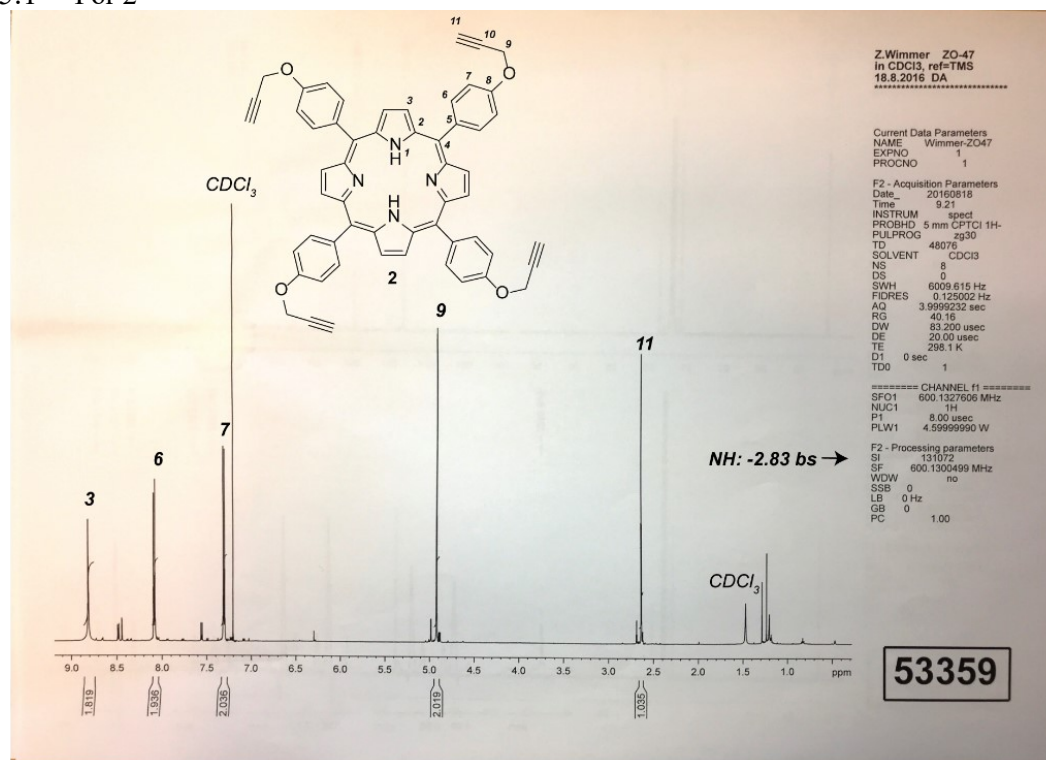


Figure S4.  $^1\text{H}$ -NMR (600 MHz,  $\text{CDCl}_3$ ) of 2.

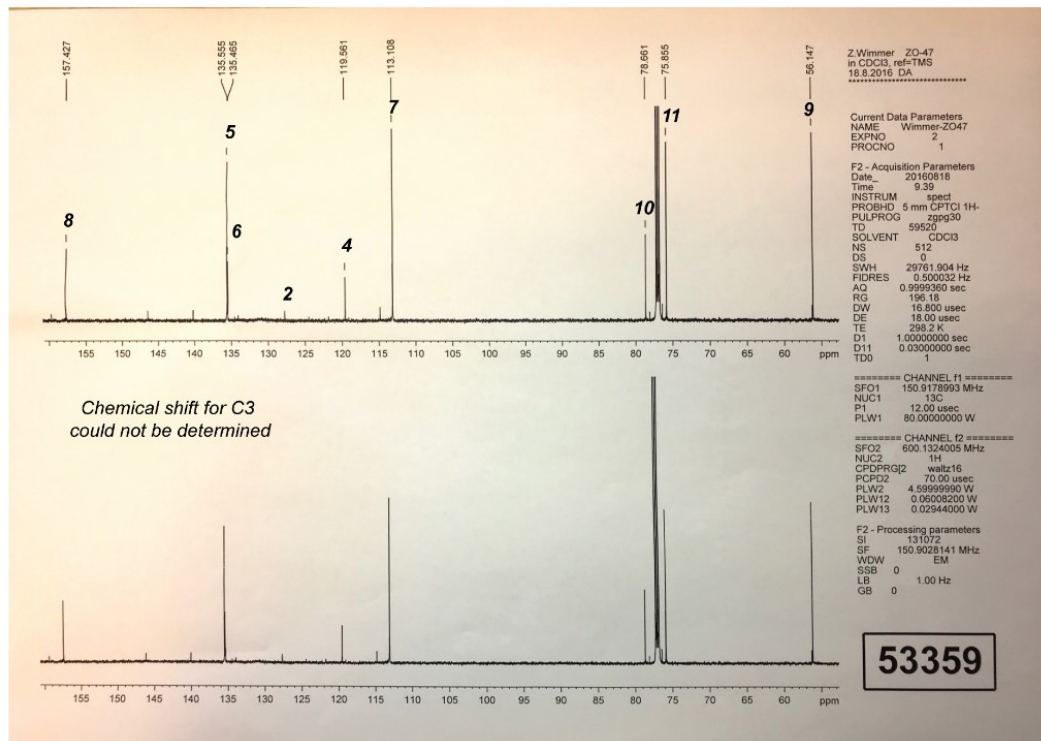


Figure S5.  $^{13}\text{C}$ -NMR (150 MHz,  $\text{CDCl}_3$ ) of 2.

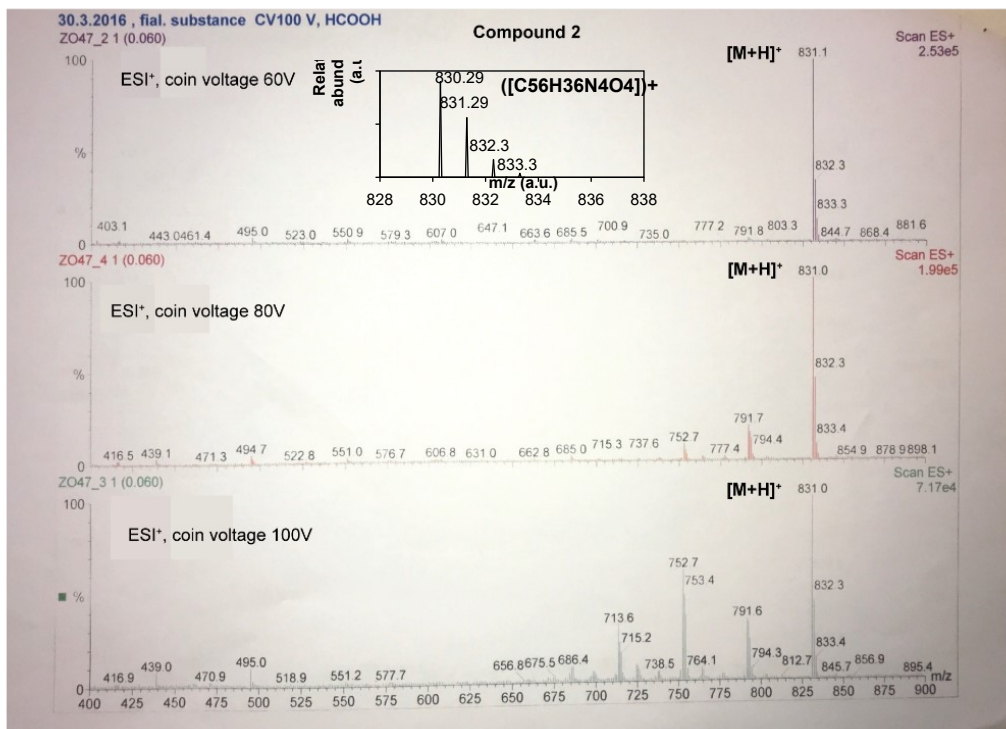


Figure S6. ESI-MS of **2**.

## 5.2 Por 3

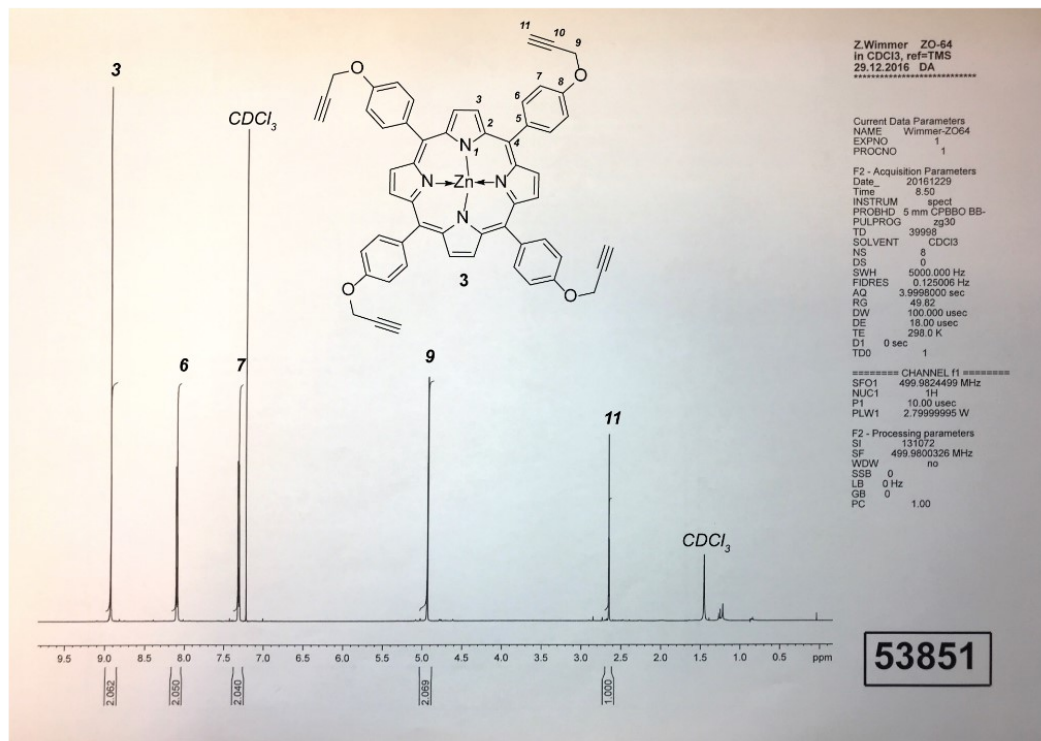


Figure S7.  $^1\text{H}$ -NMR (600 MHz,  $\text{CDCl}_3$ ) of **3**.

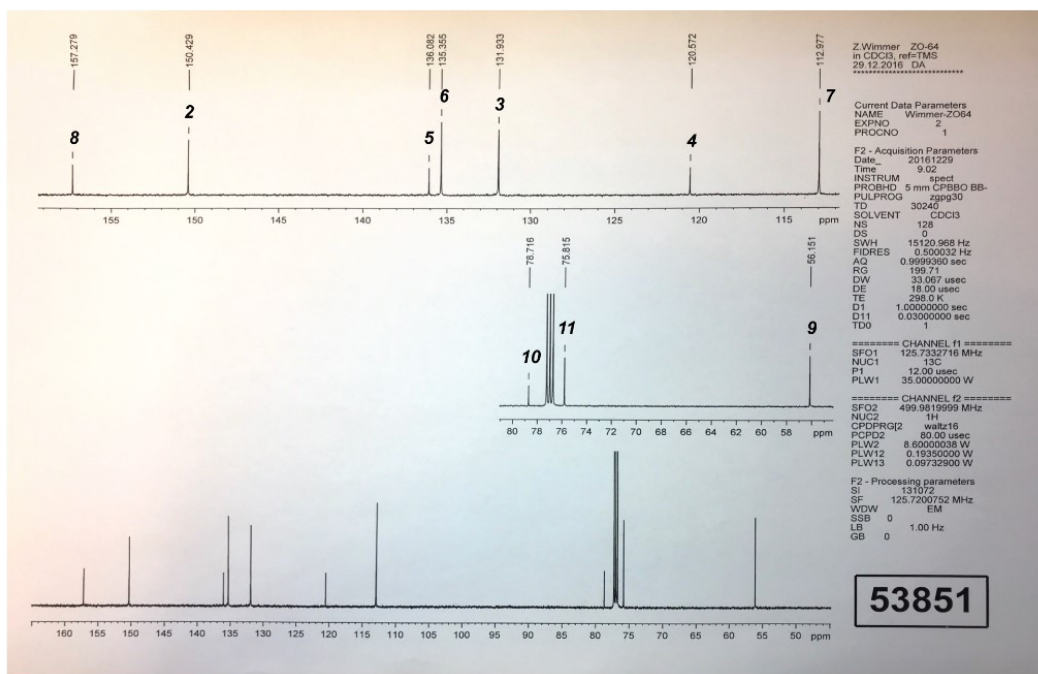


Figure S8. <sup>13</sup>C-NMR (150 MHz, CDCl<sub>3</sub>) of **3**.

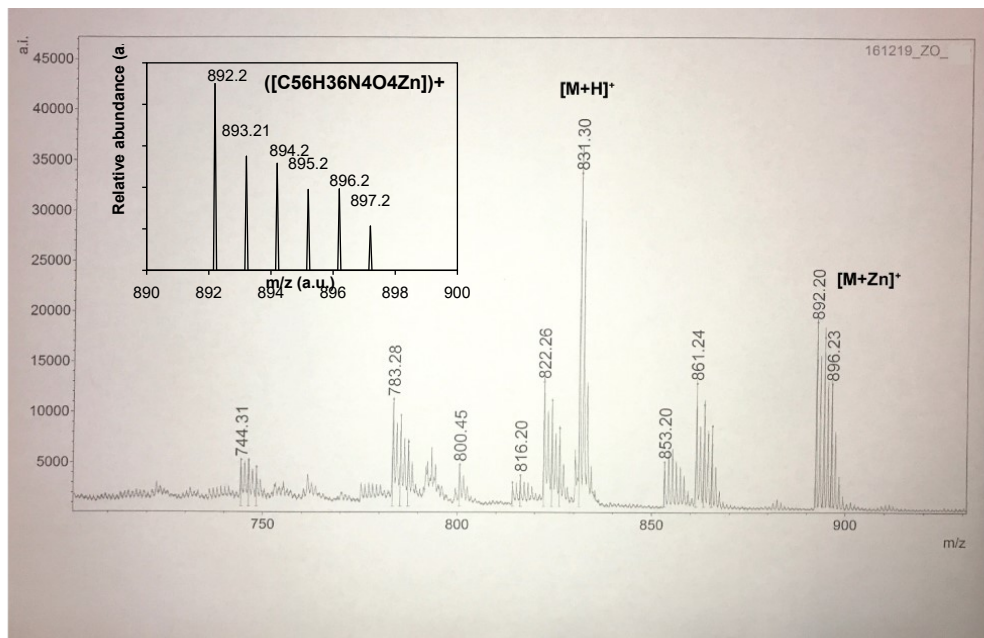


Figure S9. ESI-MS of **3**.

### 5.3 Por 4

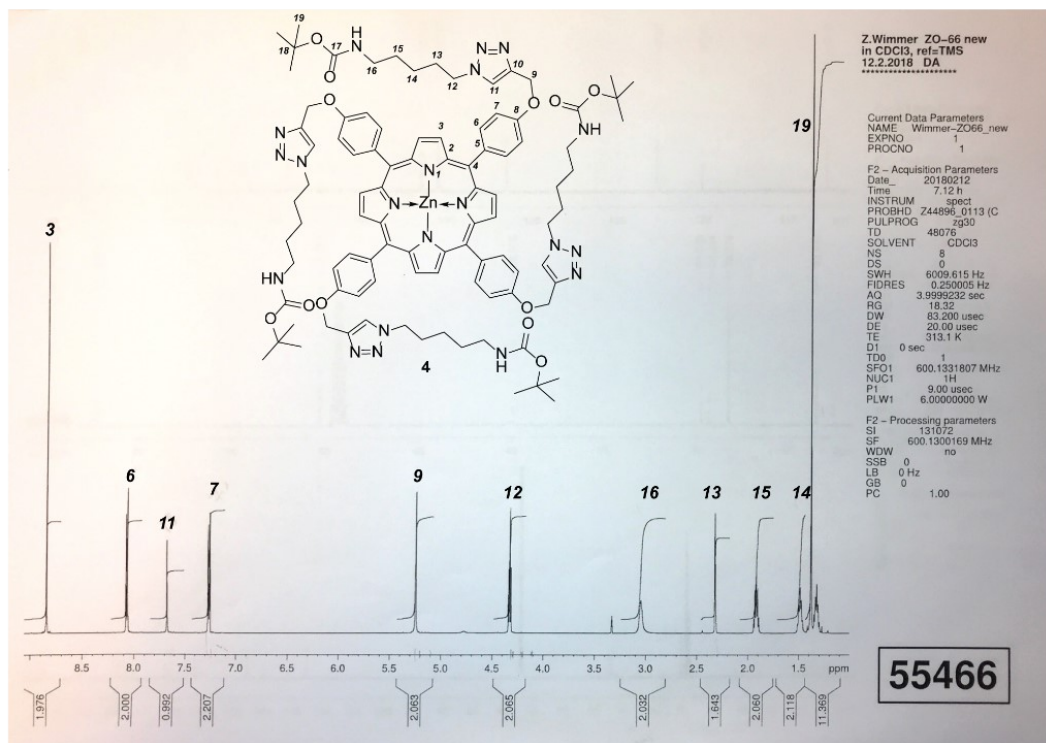


Figure S10. <sup>1</sup>H-NMR (600 MHz, CDCl<sub>3</sub>) of 4.

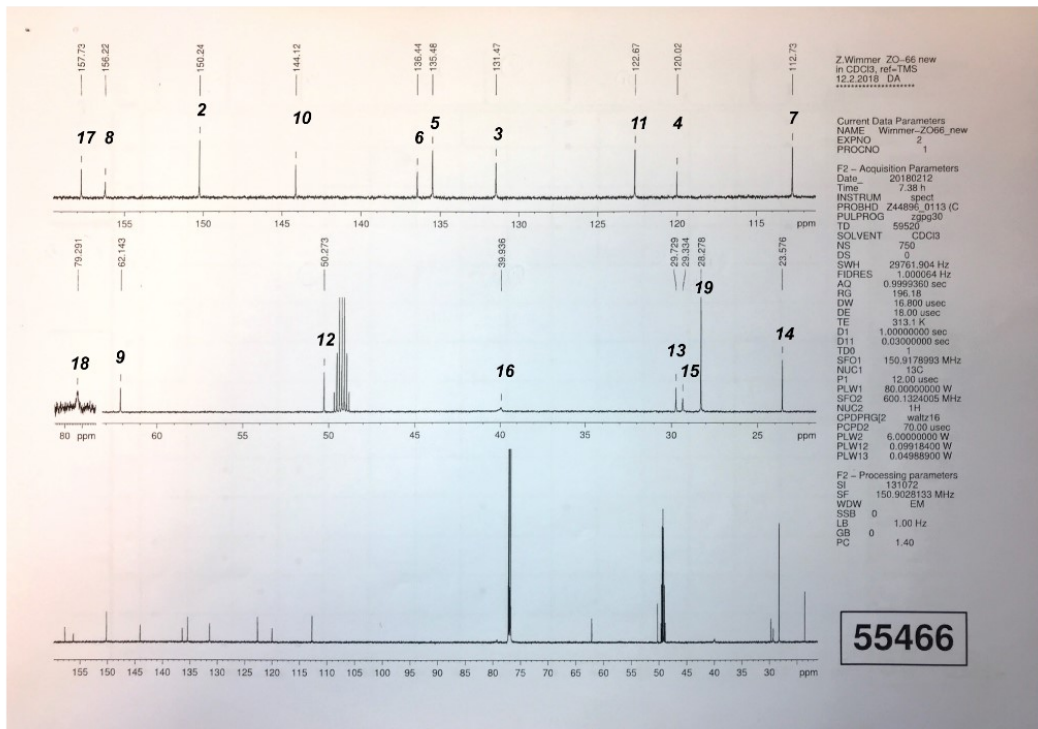


Figure S11. <sup>13</sup>C-NMR (150 MHz, CDCl<sub>3</sub>) of 4.

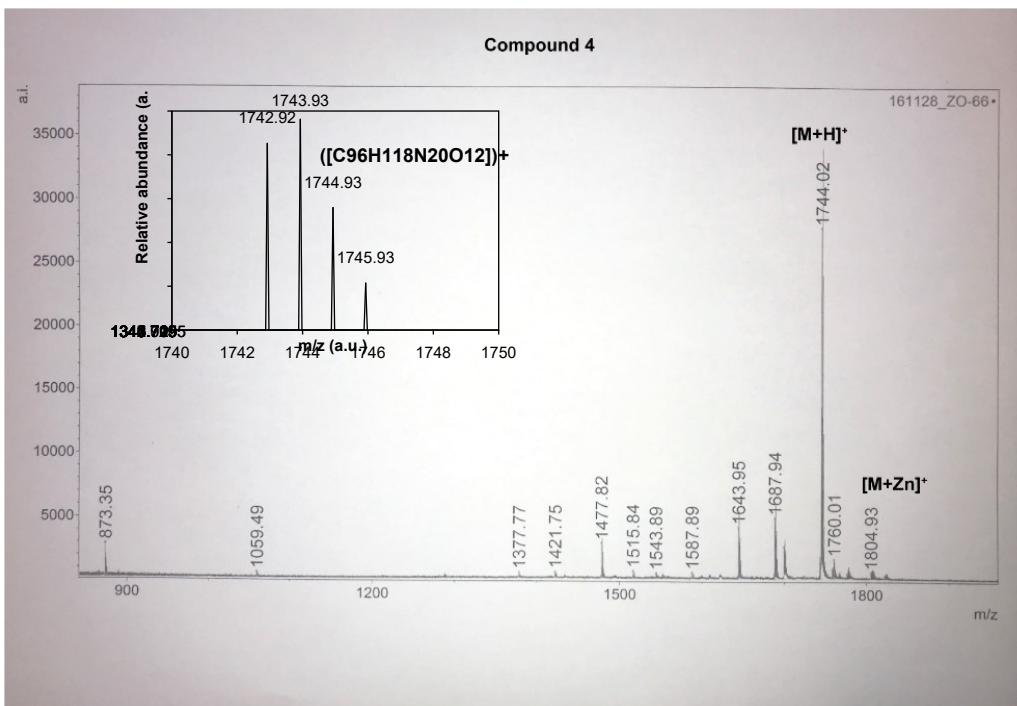


Figure S12. MALDI-TOF of 4.

#### 5.4 Por 1

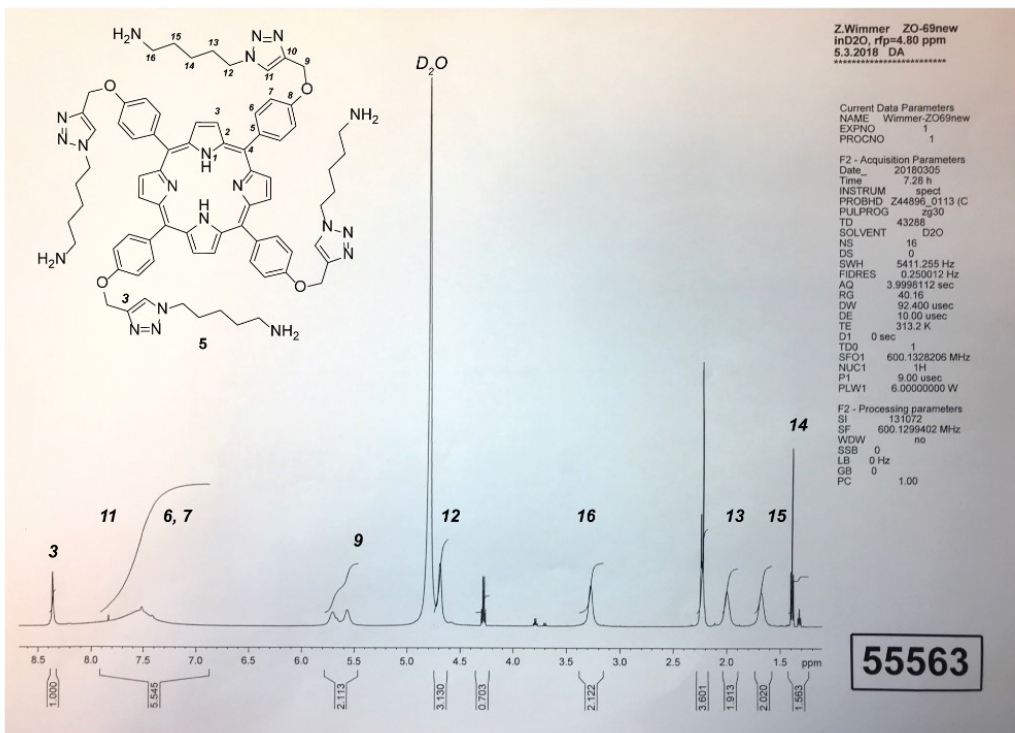


Figure S13. <sup>1</sup>H-NMR (600 MHz, D<sub>2</sub>O) of 1.

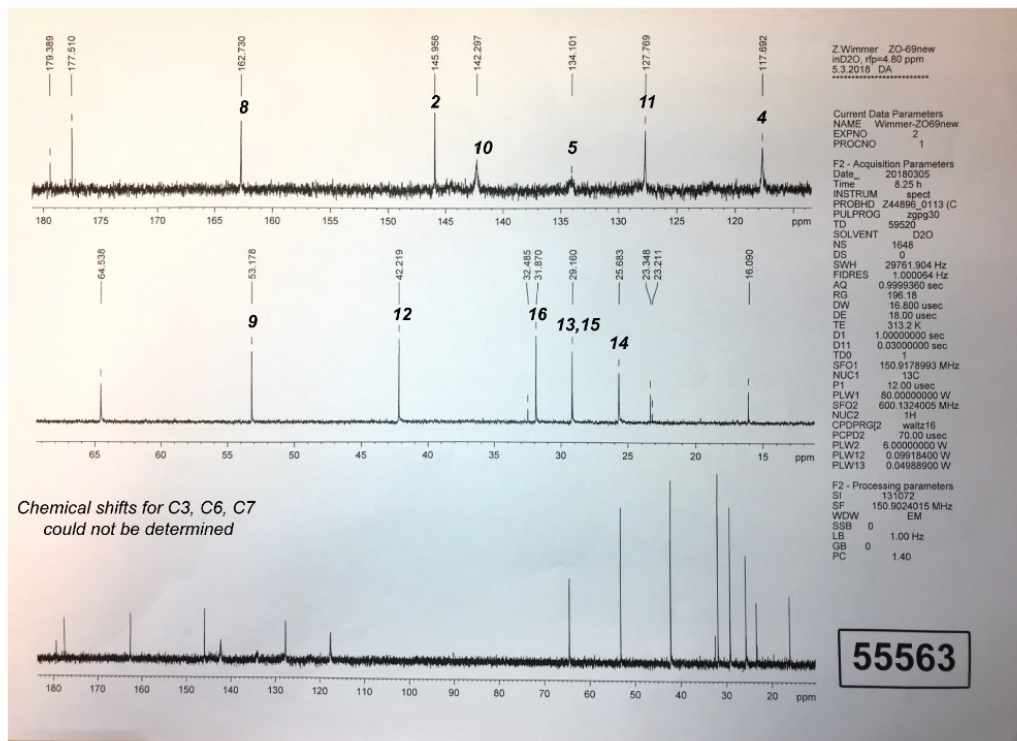


Figure S14.  $^{13}\text{C}$ -NMR (150 MHz,  $\text{D}_2\text{O}$ ) of 1.

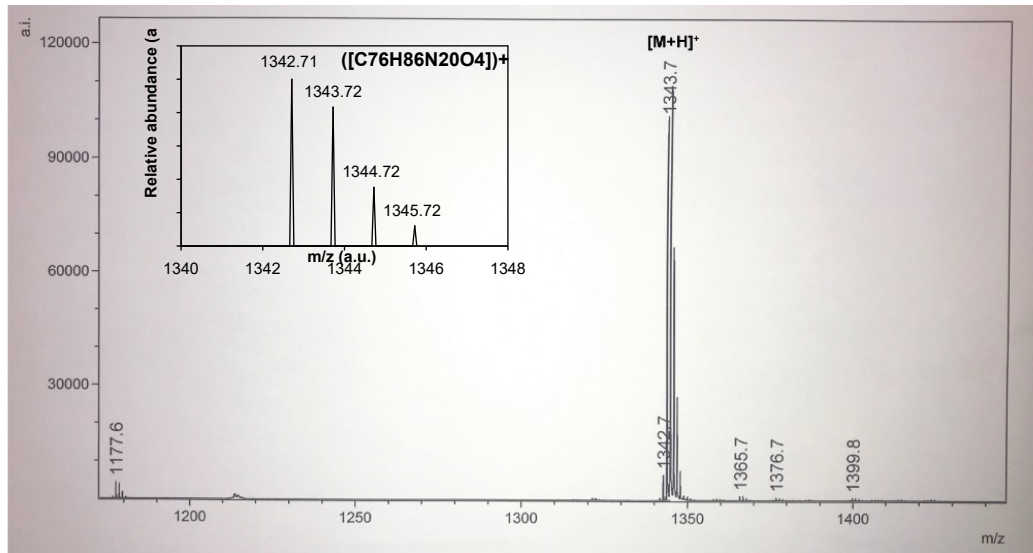


Figure S15. MALDI-TOF of 1.

## 5.5 Intermediate 5

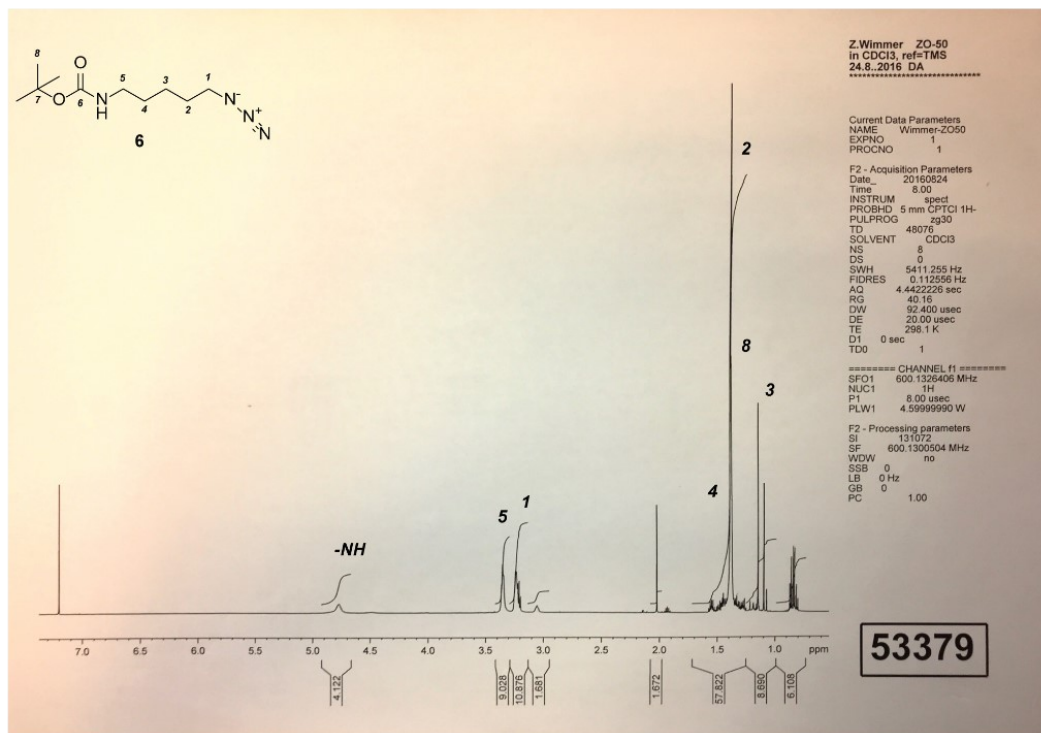


Figure S16. <sup>1</sup>H-NMR (600 MHz, CDCl<sub>3</sub>) of **5**.

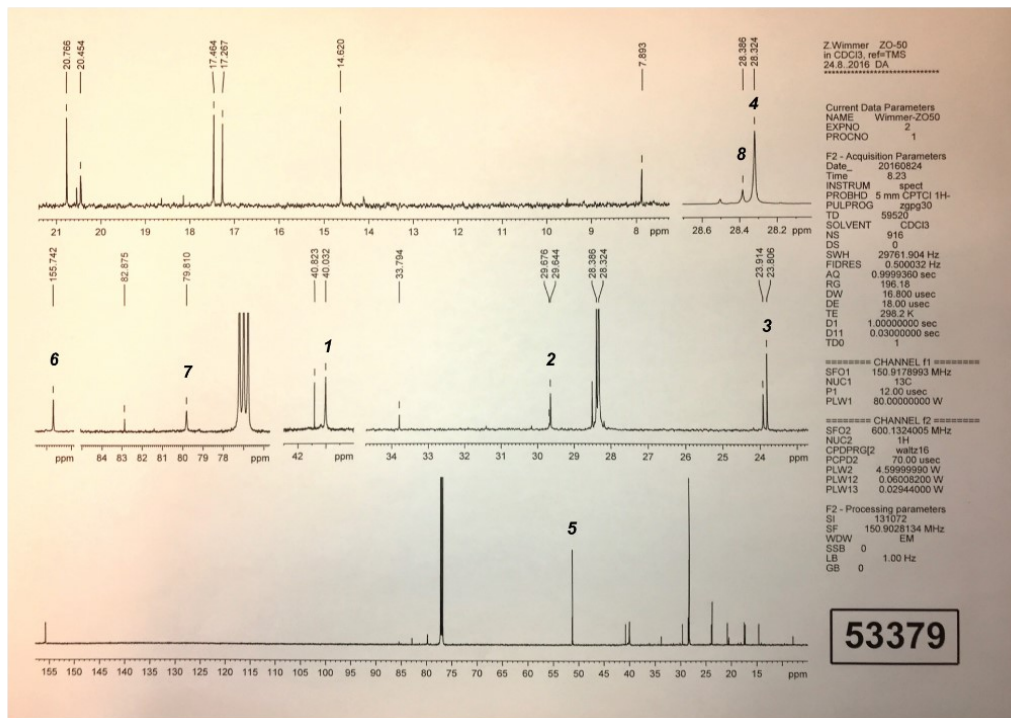


Figure S17. <sup>13</sup>C-NMR (150 MHz, CDCl<sub>3</sub>) of **5**.

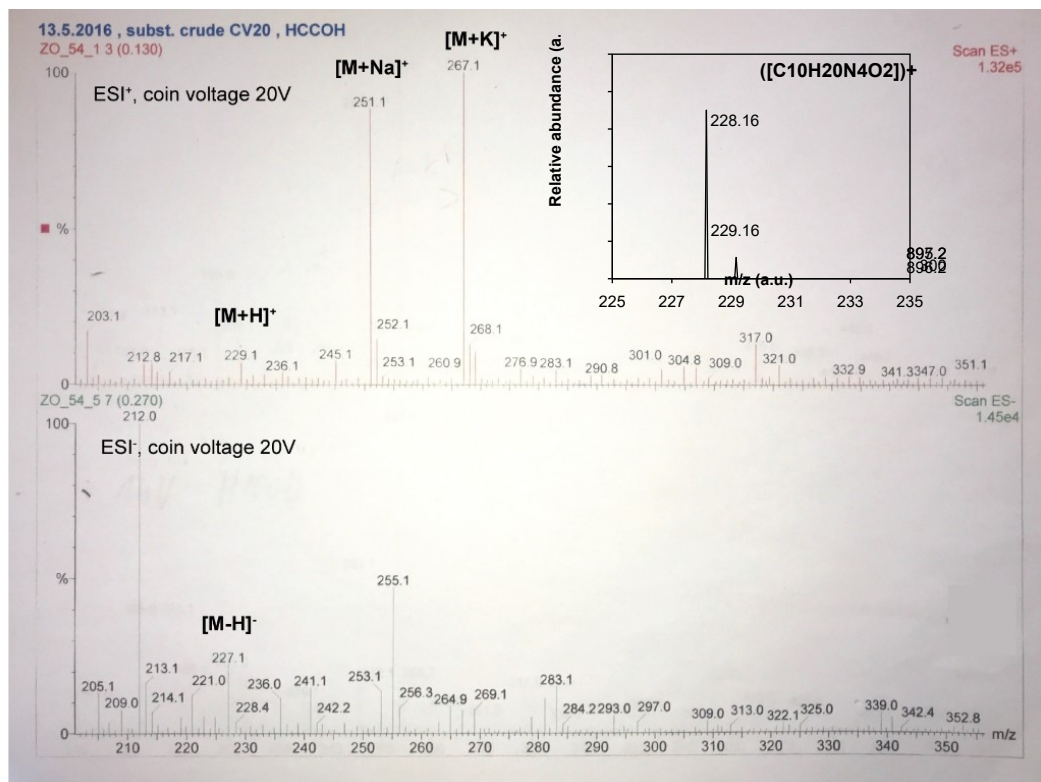


Figure S18. ESI-MS of **5**.